**The Compact Muon Solenoid Experiment**

# CMS Note
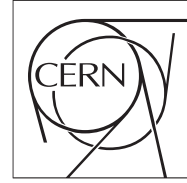
# A Search For New Physics in Z + Jets + MET using MET Templates

D. Barge, C. Campagnari, P. Kalavase, D. Kovalskyi, V. Krutelyov, J. Ribnik

*University of California, Santa Barbara, USA*

W. Andrews, G. Cerati, D. Evans, F. Golf, I. MacNeill, S. Padhi, Y. Tu, F. Würthwein, A. Yagil, J. Yoo

*University of California, San Diego, USA*

L. Bauerdick, I. Bloch, K. Burkett, I. Fisk, Y. Gao, O. Gutsche, B. Hooberman, S. Jindariani

*Fermi National Accelerator Laboratory, Batavia, Illinois, USA*

**Abstract**

We search for new physics in the dilepton final state of $Z$ plus two or more jets plus missing transverse energy (MET) in the $\sqrt{s} = 7$ TeV data in 2011 (204 pb$^{-1}$). The $Z$ boson is reconstructed in its decay to $e^+e^-$ or $\mu^+\mu^-$, and the search regions are defined as MET $\geq$ 100 GeV (loose signal region) and MET $\geq$ 200 GeV (tight signal region). We use data driven techniques to predict the standard model background in these search regions. Contributions from Drell-Yan production combined with detector mis-measurements that produce fake MET are modeled via MET templates based on photon plus jets events. Top pair production background, as well as other backgrounds for which the lepton flavors are uncorrelated, are modeled via $e^{\pm}\mu^{\mp}$ subtraction.

# Contents

# 1 Introduction

In this note we describe a search for new physics in the 2011 opposite sign isolated dilepton sample ($ee$, $e\mu$, and $\mu\mu$). The main sources of high $P_T$ isolated dileptons at CMS are Drell Yan and $t\bar{t}$ . Here we concentrate on dileptons with invariant mass consistent with $Z \to ee$ and $Z \to \mu\mu$. A separate search for new physics in the non-$Z$ sample is described in [1].

We search for new physics in the final state of $Z$ plus two or more jets plus missing transverse energy (MET). We reconstruct the $Z$ boson in its decay to $e^+e^-$ or $\mu^+\mu^-$. Our search regions are defined as MET $\geq$ 100 GeV (loose signal region) and MET $\geq$ 200 GeV (tight signal region), and two or more jets. We use data driven techniques to predict the standard model background in these search regions. Contributions from Drell-Yan production combined with detector mis-measurements that produce fake MET are modeled via MET templates based on photon plus jets events. Top pair production backgrounds, as well as other backgrounds for which the lepton flavors are uncorrelated such as WW and DY$\to \tau\tau$, are modeled via $e^\pm \mu^\mp$ subtraction.

As leptonically decaying $Z$ bosons is a signature that has very little background, they provide a clean final state in which to search for new physics. Because new physics is expected to be connected to the Standard Model Electroweak sector, it is likely that new particles will couple to W and Z bosons. For example, in mSUGRA, low $M_{1/2}$ can lead to a significant branching fraction for $\chi_2^0 \to Z\chi_1^0$. In addition, we are motivated by the existence of dark matter to search for new physics with MET. Enhanced MET is a feature of many new physics scenarios, and R-parity conserving SUSY again provides a popular example. The main challenge of this search is therefore to understand the tail of the fake MET distribution in $Z$ plus jets events.

The basic idea of the MET template method [2][3] is to measure the MET distribution in a control sample which has no true MET and a similar topology to the signal events. In our case, we choose a photon sample with two or more jets as the control sample. Both the control sample and signal sample consist of a well measured object (either a photon or a leptonically decaying $Z$), which recoils against a system of hadronic jets. In both cases, the instrumental MET is dominated by mismeasurements of the hadronic system.

This note is organized as follows. In Sections 2 and 3.1 we start by describing the triggers and datasets used, followed by the detailed object definitions (electrons, muons, photons, jets, MET) and event selection which is described in Section 3. We define a preselection and compare data vs. MC yields passing this preselection in Section 4. We then define the signal regions and show the number of observed events and MC expected yields in Section 5. Section 6 then introduces the MET template method and discusses its derivation in some detail, followed by a demonstration in Section 7 that the method works in Monte Carlo. Section 8 introduces the top background estimate based on opposite flavor subtraction, and contributions from other backgrounds are discussed in Section 9. Section 10 shows the results for applying these methods in data. We analyze the systematic uncertainties in the background prediction in Section 11 and proceed to calculate an upper limit on the non SM contributions to our signal regions in Section 12. In Section 14 we calculate upper limits on the quantity $\sigma \times BF \times A$, assuming efficiencies and uncertainties from sample benchmark SUSY processes. We conclude in Section 15.

# 2 Datasets

## 2.1 Datasets

We use the May 10 ReReco data for both leptons and photons.

For selecting the dilepton sample, the following datasets are used (the pythia DY samples are used only for generator level Z mass values less than 50 to avoid overlap with the madgraph DYJets sample):

- Data

  - /DoubleElectron/Run2011A-May10ReReco-v1/AOD

  - /DoubleMu/Run2011A-May10ReReco-v1/AOD

  - /MuEG/Run2011A-May10ReReco-v1/AOD

- Monte Carlo

50  – /DYJetsToLL_TuneD6T_M-50_7TeV-madgraph-tauola/Spring11-PU_S1_START311_V1G1-v1/AODSI

51  – /TTJets_TuneZ2_7TeV-madgraph-tauola/Spring11-PU_S1_START311_V1G1-v1/AODSIM

52  – /WJetsToLNu_TuneZ2_7TeV-madgraph-tauola/Spring11-PU_S1_START311_V1G1-v1/AODSIM

53  – /WWTo2L2Nu_TuneZ2_7TeV-pythia6/Spring11-PU_S1_START311_V1G1-v1/AODSIM

54  – /WZtoAnything_TuneZ2_7TeV-pythia6-tauola/Spring11-PU_S1_START311_V1G1-v1/AODSIM

55  – /ZZtoAnything_TuneZ2_7TeV-pythia6-tauola/Spring11-PU_S1_START311_V1G1-v1/AODSIM

56  – /TToBLNu_TuneZ2_s-channel_7TeV-madgraph/Spring11-PU_S1_START311_V1G1-v1/AODSIM

57  – /TToBLNu_TuneZ2_t-channel_7TeV-madgraph/Spring11-PU_S1_START311_V1G1-v1/AODSIM

58  – /TToBLNu_TuneZ2_tW-channel_7TeV-madgraph/Spring11-PU_S1_START311_V1G1-v1/AODSIM

59  – Pythia samples:

60  – /DYToEE_M-20_CT10_TuneZ2_7TeV-powheg-pythia/Spring11-PU_S1_START311_V1G1-v1/AODSIM

61  – /DYToMuMu_M-20_CT10_TuneZ2_7TeV-powheg-pythia/Spring11-PU_S1_START311_V1G1-v1/AODSI

62  – /DYToTauTau_M-20_CT10_TuneZ2_7TeV-powheg-pythia-tauola/Spring11-PU_S1_START311_V1G1

63  – /DYToEE_M-10To20_TuneZ2_7TeV-pythia6/Spring11-PU_S1_START311_V1G1-v1/AODSIM

64  – /DYToMuMu_M-10To20_TuneZ2_7TeV-pythia6/Spring11-PU_S1_START311_V1G1-v1/AODSIM

65  For the creation of photon templates, we use:

66  • /Photon/Run2011A-May10ReReco-v1/AOD

67  The integrated luminosity used corresponds to 204 pb$^{-1}$, and the JSON used is the official May 10 ReReco
68  JSON:
69  Cert_160404-163869_7TeV_May10ReReco_Collisions11_JSON.txt

# 3  Selection

## 3.1  Triggers

72  For data, we use a cocktail of unprescaled double lepton triggers. An event in the $ee$ final state is required
73  to pass at least one double electron trigger, a $\mu\mu$ event is required to pass at least one double muon trigger,
74  while an $e\mu$ event is required to pass at least one $e - \mu$ cross trigger. $e\mu$ events are retained in a control
75  sample used to estimate the ttbar contribution as described in Section 8.

76  The list of triggers used for selecting dilepton events can be found in Appendix A.1 for which the ap-
77  proximate efficiencies are 90% ($\mu\mu$), 95% ($e\mu$), 100% ($ee$).

78  Triggers used for creation of photon templates are listed in Section 6.

## 3.2  Event Selections

80  These event selections are implemented following the recommendation of PVT.

81  • If at least 10 tracks are present, at least 25% of them must be high purity.

82  • At least one primary vertex which passes the following selections is required:

83  – Not fake
84  – At least 5 degrees of freedom
85  – $\rho < 2$ cm
86  – $|z| < 24$ cm

## 3.3 Lepton Selection

Because $Z \rightarrow l^+l^-$ (where $l$ is an electron or muon) is a final state with very little background after a Z mass requirement is applied to the leptons, we restrict ourselves to events in which the Z boson decays to electrons or muons only. Therefore two same flavor, opposite sign leptons passing the ID described below are required in each event.

- $P_T > 20$ GeV

- Opposite sign, same flavor ($e^{\pm}\mu^{\mp}$ events are retained in a control sample used to estimate the ttbar contribution)

- Dilepton invariant mass is consistent with the Z mass: between 81 and 101 GeV

- Electron ID

  - $|\eta| < 2.5$
  - VBTF 90 ID from the Egamma group[6], tightened to match HLT requirements CaloIdT+TrkIdVL which includes: [7]
    * H/E < 0.1 (0.075), $\sigma_{i\eta i\eta} < 0.011$ (0.031) in barrel (endcap)
    * $d\eta < 0.01$ (0.01), $d\phi < 0.15$ (0.1) in barrel (endcap)
  - $|d_0| < 0.04$ (with respect to the first DA primary vertex)
  - $|d_z| < 1.0$ (with respect to the first DA primary vertex)
  - Isolation: The sum of the $P_T$ of tracks and the transverse energy in both calorimeters in a cone of $dR = 0.3$ divided by the $P_T$ of the electron is required to be less than 0.15. In the barrel only, a pedestal of 1 GeV is subtracted from the ECAL energy.
  - No muon is allowed to be within $dR < 0.1$ of the electron
  - No more than one missing inner tracker hit [8]
  - In order to reject electrons from conversions, we veto electrons with a reconstructed conversion vertex [9]
  - Supercluster $E_T > 10$ GeV

- Muon ID

  - Muon $|\eta| < 2.4$
  - Muon global fit is required to have $\chi^2$ divided by number of degrees of freedom less than 10
  - Required to be both global and tracker
  - Silicon track is required to have at least 11 hits
  - The ECAL energy in the calorimeter tower traversed by the muon cannot exceed 4 GeV
  - The HCAL energy in the calorimeter tower traversed by the muon cannot exceed 6 GeV
  - Must have at least one stand-alone hit
  - $|d_0| < 0.02$ (with respect to the first DA primary vertex)
  - $|d_z| < 1.0$ (with respect to the first DA primary vertex)
  - Relative transverse momentum error of silicon track used for muon fit is $\delta(p_T)/p_T < 0.1$
  - The muon is required to be a PF muon whose $P_T$ is no more than 1 GeV different than the reco muon (to ensure consistency with PF MET)
  - The same isolation requirement is applied as in the electron case (but no pedestal is subtracted from the ECAL energy).

- Dilepton Selection

  - If more than 1 pair of leptons passing the above selection is present in the event, choose the pair with mass closest to $M_Z$. These leptons are referred to as the Z hypothesis leptons.

6

## 3.4 Photons

As will be explained later, it is not essential that we select real photons. What is needed are jets that are predominantly electromagnetic, well measured in the ECAL, and hence less likely to contribute to fake MET. We select "photons" with:

- $P_T > 22$ GeV

- $|\eta| < 2$

- $H/E < 0.1$

- There must be a pfjet of $P_T > 10$ GeV which passes loose particle flow jet identification requirements matched to the photon within $dR < 0.3$. The matched jet is required to have a neutral electromagnetic energy fraction of at least 90%.

- A jet encompassing a photon has to have energy greater than or equal to that of the photon within its cone. We require that the pfjet $P_T$ matched to the photon satisfy pfjet $P_T$ - photon $P_T >$ -5 GeV. This removes a few cases in which "overcleaning" of an ECAL recHit generated fake MET.

## 3.5 MET

We use pfMET, henceforth referred to simply as "MET."

## 3.6 Jets

- PF jets

- $|\eta| < 3.0$

- L2L3 corrected

- L1Fastjet corrected to account for pile up

- $P_T > 30$ GeV for Njet counting, $P_T > 15$ GeV for sum jet $P_T$ counting

- For the creation of photon templates, the jet matched to the photon passing the photon selection described above is vetoed

- For the dilepton sample, jets are vetoed if they are within $dR < 0.4$ from any lepton $P_T > 20$ GeV passing analysis selection

# 4 Preselection yields

Based on the event and trigger selections described in Section 3, we define a preselection as follows:

- Number of jets $\geq 2$

- Same flavor dileptons (opposite flavor yields will be shown since they are used in data for $t\bar{t}$ background estimation)

- Dilepton mass within 10 GeV of the Z mass

The resulting dilepton mass spectra for the $ee$ and $\mu\mu$ final states are shown in Figure 1.

The data yields and the MC predictions are given in Table 1.

The MC yields are normalized to 204 pb$^{-1}$ using the cross-sections from Reference [10] assuming 100% trigger efficiency . As anticipated, the MC predicts that the preselection is dominated by Z+jets in the same-flavor case and by $t\bar{t}$ in the opposite-flavor case. The data yield is in reasonable agreement with the predictions for the $ee$, $\mu\mu$ and $e\mu$ channels. We also show the LO yields for the LM4 and LM8 processes, which are benchmark SUSY processes in which $Z$ bosons are produced via cascade decays of SUSY particles.
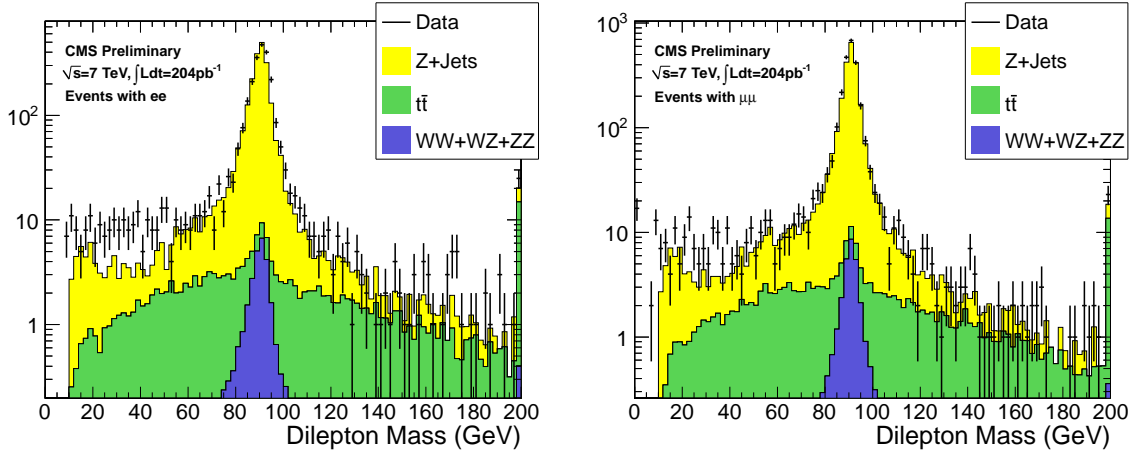
Figure 1: Dilepton mass distribution for events passing the pre-selection for 204 pb$^{-1}$ in the $ee$ (left) and $\mu\mu$ (right) final states. Backgrounds from single top and $W$+jets are omitted since they are negligible.

Table 1: Data and Monte Carlo yields for the preselection for 204 pb$^{-1}$. The NLO yields for the SUSY benchmark processes LM4 and LM8 are also shown.

| Sample | $ee$ | $\mu\mu$ | $e\mu$ | tot |
|---|---|---|---|---|
| Z+Jets | $1840.566 \pm 21.213$ | $2088.019 \pm 22.592$ | $1.467 \pm 0.599$ | $3930.052 \pm 30.996$ |
| $t\bar{t}$ | $24.515 \pm 0.860$ | $25.965 \pm 0.885$ | $51.295 \pm 1.244$ | $101.775 \pm 1.753$ |
| WJets | $0.852 \pm 0.603$ | $0.000 \pm 0.000$ | $0.426 \pm 0.426$ | $1.278 \pm 0.738$ |
| WW | $0.217 \pm 0.043$ | $0.442 \pm 0.061$ | $0.593 \pm 0.070$ | $1.252 \pm 0.102$ |
| WZ | $13.947 \pm 0.157$ | $16.001 \pm 0.168$ | $0.111 \pm 0.014$ | $30.059 \pm 0.230$ |
| ZZ | $10.005 \pm 0.076$ | $11.364 \pm 0.082$ | $0.022 \pm 0.004$ | $21.391 \pm 0.112$ |
| Single Top | $0.725 \pm 0.057$ | $0.778 \pm 0.059$ | $1.694 \pm 0.088$ | $3.196 \pm 0.120$ |
| Total MC | $1890.827 \pm 21.240$ | $2142.569 \pm 22.610$ | $55.607 \pm 1.450$ | $4089.003 \pm 31.056$ |
| Data | 2051 | 2250 | 67 | 4368 |
| LM4 | $2.027 \pm 0.060$ | $2.175 \pm 0.062$ | $0.291 \pm 0.023$ | $4.493 \pm 0.089$ |
| LM8 | $0.889 \pm 0.025$ | $1.004 \pm 0.026$ | $0.273 \pm 0.014$ | $2.167 \pm 0.038$ |

# 5 Definition of the signal regions

We define signal regions to look for possible new physics contributions by adding the requirement of large MET to the preselection. Our choice of MET requirements to define the signal regions is driven by the MET distributions expected from $Z$ and $t\bar{t}$ MC with the preselection applied, as shown in Fig. 2. The integrated luminosity of the $Z$ MC is approximately 834 pb$^{-1}$, and that of the $t\bar{t}$ sample is approximately 6.8 fb$^{-1}$.

We define two signal regions for our search:

- MET > 100GeV (loose signal region):

   In this region of MET there is a small contribution from the tail of the MET distribution in $Z$ plus jets events. The bulk of the events in this region are from $t\bar{t}$ events where the leptons happen to be in the $Z$ mass window.

   The MC and data yields for this signal region are given in Table 2 and the dilepton mass distributions are shown in Fig. 3.

- MET > 200GeV (tight signal region): This signal region was selected by picking a region where the SM expectation is very low. At this kinematical region the dominant background contribution is expected to be from $t\bar{t}$ .

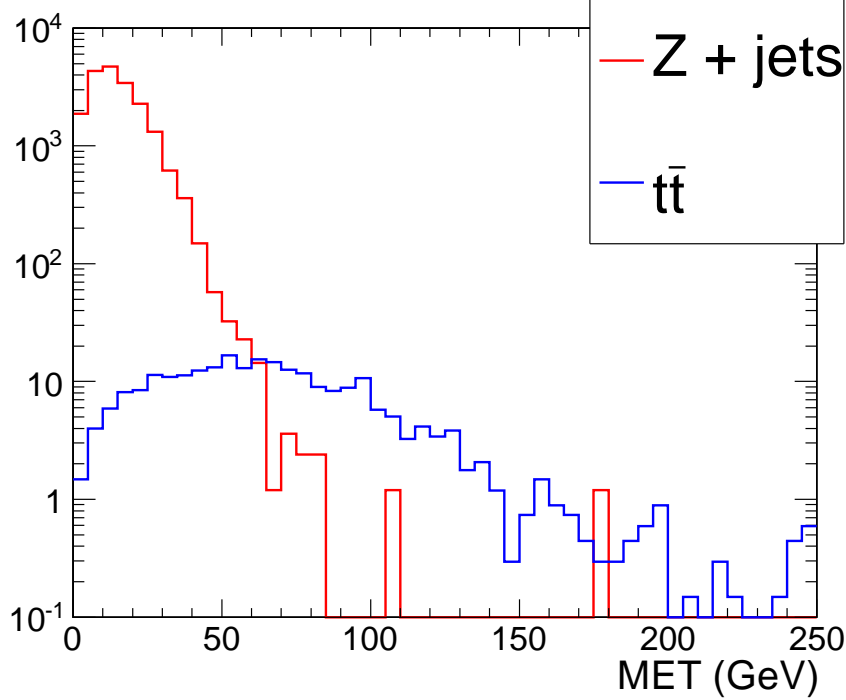   The MC and data yields for this signal region are given in Table 3.

Figure 2: Distributions of MET in $Z$ and $t\bar{t}$ MC normalized to 1 fb$^{-1}$.

In the two signal regions above, the dominant background is $t\bar{t}$. However, it is still essential to have a data driven estimation of the $Z$ contribution in the signal regions to demonstrate that we understand our background composition. This is important both in case when an excess is observed or when placing a limit on new physics.

The data driven technique used to predict the missing transverse energy accompanying a $Z$ event is described in Section 6.

To estimate the $t\bar{t}$ background we will use the opposite flavor subtraction described in Section 8.

Table 2: Data and Monte Carlo yields for the loose signal region MET > 100 GeV for 204 pb$^{-1}$.

| Sample | $ee$ | $\mu\mu$ | $e\mu$ | tot |
|---|---|---|---|---|
| Z+Jets | $0.489 \pm 0.346$ | $0.000 \pm 0.000$ | $0.000 \pm 0.000$ | $0.489 \pm 0.346$ |
| $t\bar{t}$ | $3.714 \pm 0.335$ | $4.317 \pm 0.361$ | $8.454 \pm 0.505$ | $16.485 \pm 0.705$ |
| WJets | $0.000 \pm 0.000$ | $0.000 \pm 0.000$ | $0.000 \pm 0.000$ | $0.000 \pm 0.000$ |
| WW | $0.025 \pm 0.014$ | $0.058 \pm 0.022$ | $0.100 \pm 0.029$ | $0.184 \pm 0.039$ |
| WZ | $0.155 \pm 0.017$ | $0.144 \pm 0.016$ | $0.004 \pm 0.002$ | $0.303 \pm 0.023$ |
| ZZ | $0.088 \pm 0.007$ | $0.096 \pm 0.007$ | $0.000 \pm 0.000$ | $0.184 \pm 0.010$ |
| Single Top | $0.102 \pm 0.021$ | $0.133 \pm 0.024$ | $0.256 \pm 0.034$ | $0.490 \pm 0.047$ |
| Total MC | $4.572 \pm 0.482$ | $4.749 \pm 0.363$ | $8.814 \pm 0.507$ | $18.134 \pm 0.788$ |
| Data | 7 | 7 | 12 | 26 |
| LM4 | $1.522 \pm 0.052$ | $1.603 \pm 0.053$ | $0.232 \pm 0.020$ | $3.356 \pm 0.077$ |
| LM8 | $0.597 \pm 0.020$ | $0.686 \pm 0.022$ | $0.219 \pm 0.012$ | $1.502 \pm 0.032$ |

# 6  MET Templates

The premise of this data driven technique is that MET in $Z$ plus jets events is produced by the hadronic recoil system and *not* by the leptons making up the $Z$. Therefore, the basic idea of the MET template method is to measure the MET distribution in a control sample which has no true MET and the same
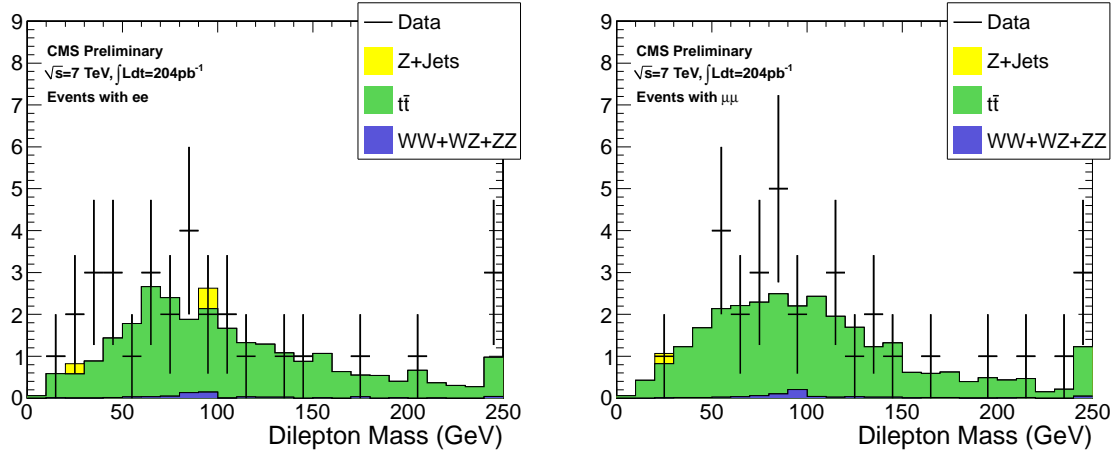
Figure 3: Dilepton mass distribution for events passing the pre-selection and MET > 100 GeV for 204 pb$^{-1}$ in the $ee$ (left) and $\mu\mu$ (right) final states. Backgrounds from single top and $W$+jets are omitted since they are negligible.

Table 3: Data and Monte Carlo yields for the tight signal region MET > 200 GeV for 204 pb$^{-1}$.

| Sample | $ee$ | $\mu\mu$ | $e\mu$ | tot |
|---|---|---|---|---|
| Z+Jets | $0.000 \pm 0.000$ | $0.000 \pm 0.000$ | $0.000 \pm 0.000$ | $0.000 \pm 0.000$ |
| $t\bar{t}$ | $0.181 \pm 0.074$ | $0.181 \pm 0.074$ | $0.483 \pm 0.121$ | $0.845 \pm 0.160$ |
| WJets | $0.000 \pm 0.000$ | $0.000 \pm 0.000$ | $0.000 \pm 0.000$ | $0.000 \pm 0.000$ |
| WW | $0.000 \pm 0.000$ | $0.008 \pm 0.008$ | $0.008 \pm 0.008$ | $0.017 \pm 0.012$ |
| WZ | $0.025 \pm 0.007$ | $0.021 \pm 0.006$ | $0.000 \pm 0.000$ | $0.046 \pm 0.009$ |
| ZZ | $0.013 \pm 0.003$ | $0.013 \pm 0.003$ | $0.000 \pm 0.000$ | $0.026 \pm 0.004$ |
| Single Top | $0.000 \pm 0.000$ | $0.013 \pm 0.008$ | $0.009 \pm 0.006$ | $0.022 \pm 0.010$ |
| LM4 | $0.922 \pm 0.040$ | $0.969 \pm 0.041$ | $0.128 \pm 0.015$ | $2.019 \pm 0.060$ |
| LM8 | $0.345 \pm 0.015$ | $0.387 \pm 0.016$ | $0.144 \pm 0.010$ | $0.876 \pm 0.024$ |
| Total MC | $0.219 \pm 0.074$ | $0.237 \pm 0.075$ | $0.500 \pm 0.121$ | $0.956 \pm 0.161$ |
| Data | $0$ | $2$ | $2$ | $4$ |
| LM4 | $0.922 \pm 0.040$ | $0.969 \pm 0.041$ | $0.128 \pm 0.015$ | $2.019 \pm 0.060$ |
| LM8 | $0.345 \pm 0.015$ | $0.387 \pm 0.016$ | $0.144 \pm 0.010$ | $0.876 \pm 0.024$ |

general attributes regarding fake MET as in $Z$ plus jets events. In our case, we choose a photon-like sample. These are not necessarily photons, but jets with predominantly electromagnetic energy deposition in a good fiducial volume. This ensures that they are well measured and do not contribute to fake MET.

Both the control sample and the $Z$ plus jets background consist of a well measured object (either a photon or a leptonically decaying $Z$ ) which recoils against a system of hadronic jets. The MET in these events is then dominated by mismeasurements of the hadronic system. To account for kinematic differences between the hadronic systems in the control vs. signal samples, we measure the MET distributions in the control sample in bins of the number of jets and the scalar sum of jet $P_T$ .

In order to track conditions which change over the course of data-taking (most notably the increased pile-up) and to increase the statistics at large photon $P_T$ , we use templates obtained from multiple photon triggers "stitched" together. Each photon event enters the template for the highest $P_T$ photon trigger which fired in the event. The resulting MET distributions in each bin of njets, sumjetpt and photon trigger are then normalized to unit area, yielding an array of MET templates.

Each $Z$ event is then assigned one such unit area template based on its number of jets, the scalar sum of jet $P_T$ and the $Z$ $P_T$ . The $Z$ $P_T$ enters only in choosing which bin of photon trigger to use. This is done because the $Z$ $P_T$ is the analogous variable in the $Z$ sample to the photon $P_T$ . In order to account for the different prescales of the different photon triggers (which change during running), each template is

filled with a weight equal to the prescale of the corresponding trigger. After this procedure, the templates are normalized to unity. If this is not done, the relative contribution of different parts of the photon $P_T$ specturm will not be sampled properly. In other words, this procedure corrects and smoothes the photon $P_T$ distribution. The ranges of $Z$ $P_T$ chosen for each photon trigger take into account the turn-on of the photon trigger and are shown below.

The sum of the templates for all selected $Z$ events then forms the prediction of the MET distribution for the $Z$ sample. Integrating this prediction for our signal regions thus provides a data driven prediction for the $Z$ plus jets yields in the signal regions.

While there is in principle a small contribution from $t\bar{t}$ in the $Z$ sample from which we predict the MET distribution, it is only $\approx 2.6\%$ of the total sample used (MC expectation), as shown in table 1, and the data driven prediction (see Fig. 6) estimates that the $t\bar{t}$ contribution to the loose signal region is $\approx 0.3\%$ of the total $Z$ yield. As the MET measurement in these events does not enter the MET prediction, this small non-Z contribution is negligible.

The Njet binning used is 2 jets and $\geq 3$ jets. The sum jet $P_T$ binning is defined by the boundaries 0, 30, 60, 90, 120, 150, 250, 5000 GeV. The photon triggers, and the ranges of $Z$ $P_T$ for which they are selected, are (where the "v*" stands for a verion number which increments with trigger menu changes):

- `HLT_Photon20_CaloIdVL_IsoL_v*` ($Z$ $P_T < 33$ GeV)

- `HLT_Photon30_CaloIdVL_IsoL_v*` ($33$ GeV $< Z$ $P_T < 55$ GeV)

- `HLT_Photon50_CaloIdVL_IsoL_v*` ($55$ GeV $< Z$ $P_T < 81$ GeV)

- `HLT_Photon75_CaloIdVL_IsoL_v*` ($Z$ $P_T > 81$ GeV)

The HLT requirements (as described in [7]) on the above triggers are listed in appendix A.2.

We show all the templates used in appendix B.

# 7 Closure Test of Templates in MC

The above procedure is applied to MC to test its effectiveness under 'ideal' conditions. Templates are derived from PhotonJet MC, and these templates are used to predict the MET distribution in ZJets MC. The MC samples used are:

- PhotonJet MC

    - `/G_Pt_15to30_TuneZ2_7TeV_pythia6/Spring11-PU_S1_START311_V1G1-v1/AODSIM`
    - `/G_Pt_30to50_TuneZ2_7TeV_pythia6/Spring11-PU_S1_START311_V1G1-v1/AODSIM`
    - `/G_Pt_50to80_TuneZ2_7TeV_pythia6/Spring11-PU_S1_START311_V1G1-v1/AODSIM`
    - `/G_Pt_80to120_TuneZ2_7TeV_pythia6/Spring11-PU_S1_START311_V1G1-v1/AODSIM`
    - `/G_Pt_120to170_TuneZ2_7TeV_pythia6/Spring11-PU_S1_START311_V1G1-v1/AODSIM`
    - `/G_Pt_170to300_TuneZ2_7TeV_pythia6/Spring11-PU_S1_START311_V1G1-v1/AODSIM`

- ZJet MC

    - `/DYToEE_M-20_CT10_TuneZ2_7TeV-powheg-pythia/Spring11-PU_S1_START311_V1G1-v1/AODSIM`
    - `/DYToMuMu_M-20_CT10_TuneZ2_7TeV-powheg-pythia/Spring11-PU_S1_START311_V1G1-v1/AODSI`
    - `/DYToTauTau_M-20_CT10_TuneZ2_7TeV-powheg-pythia-tauola/Spring11-PU_S1_START311_V1G1`

Good agreement between the observed and predicted MET distributions is observed, as shown in Fig. 4.

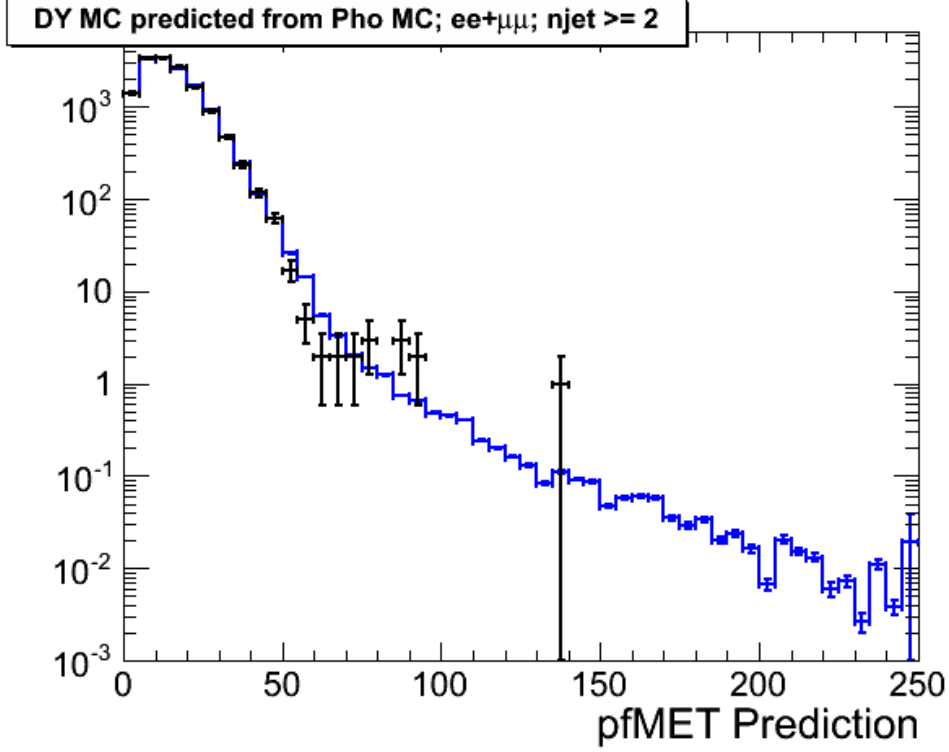| MET | > 30 GeV | > 60 GeV | > 100 GeV | > 200 |
|---|---|---|---|---|
| Z MC | 919 | 15 | 1 | 0 |
| Prediction | $950.35 \pm 2.37$ | $17.89 \pm 0.07$ | $2.44 \pm 0.02$ | $0.11 \pm 0.01$ |

Figure 4: The MET distribution in Z+jets MC (black) and prediction (blue) for Njet $\geq$ 2. Below the plot is tabulated the integral of the observed Z+jets MC MET and the predicted MET from $\gamma$+jets MC for MET > 30 GeV, > 60 GeV, and > 100 GeV, and > 200 GeV.

## 8  Top Background Estimation

The MET templates method is used to estimate the contribution of SM $Z$ production to the signal region due to the fake MET tail. However, it does not account for the $t\bar{t}$ background in which the dileptons happen to lie in the $Z$ mass window, which is accompanied by genuine MET. To estimate this contribution we use an opposite-flavor subtraction technique which takes advantage of the fact that the $t\bar{t}$ yield in the opposite-flavor final state ($e\mu$) is the same as in the same-flavor final state ($ee+\mu\mu$), modulo differences in efficiency in the $e$ vs. $\mu$ selection. Hence the $t\bar{t}$ yield in the same-flavor final state can be estimated using the corresponding yield in the opposite-flavor final state. It is important to note that other backgrounds for which the lepton flavors are uncorrelated (for example $WW$ and DY$\to \tau\tau$) will also be included in this estimate.

The simplest option is to take the $e\mu$ yield inside the $Z$ mass window and scale this to predict the $ee$ and $\mu\mu$ yields, based on $e$ and $\mu$ selection efficiencies. Only the ratio of muon to electron selection efficiency is needed, which we evaluate as $\epsilon_{\mu e} = \sqrt{\frac{N_{Z\mu\mu}}{N_{Zee}}}$. Here $N_{Zee}$ ($N_{Z\mu\mu}$) is the total number of events in the $ee$ ($\mu\mu$) final state passing the pre-selection in Section 4, without the requirement of at least 2 jets. We find $\epsilon_{\mu e} = 1.060 \pm 0.003$ (stat). (Note that in the following $\epsilon_{e\mu} = 1/\epsilon_{\mu e}$.) Systematic uncertainties on the prediction are assessed in section 11.2, and only statistical uncertainties are given in this section.

This procedure yields the following predicted yields $n_{pred}$, based on an observed yield of 12 $e\mu$ events in the loose signal region (the corresponding predictions in the tight signal region are shown in figures 7 and 8):

$$n_{pred}(\mu\mu) = \frac{1}{2}n(e\mu)\epsilon_{\mu e} = 6.36 \pm 1.84 \tag{1}$$

$$n_{pred}(ee) = \frac{1}{2}n(e\mu)\epsilon_{e\mu} = 5.66 \pm 1.63 \tag{2}$$

The predicted same flavor $t\bar{t}$ yields can be compared with the MC expectation of 4.3 ($\mu\mu$) and 3.7 ($ee$) as shown in Table 2. Due to the relatively small statistics, the errors on the predicted yields using this procedure are fairly large. To improve the statistical errors, we instead determine the $e\mu$ yield without requiring the leptons to fall in the $Z$ mass window. This yield is scaled by a factor determined from MC, $K = 0.16$, which accounts for the fraction of $t\bar{t}$ events expected to fall in the $Z$ mass window. This procedure yields the following predicted yields based on 74 observed $e\mu$ events:

$$n_{pred}(\mu\mu) = \frac{1}{2}n(e\mu)K\epsilon_{\mu e} = 6.22 \pm 0.72 \tag{3}$$

$$n_{pred}(ee) = \frac{1}{2}n(e\mu)K\epsilon_{e\mu} = 5.54 \pm 0.64 \tag{4}$$

Notice that the yields are consistent with those predicted without using $K$, but the relative statistical uncertainty is reduced by a factor of approximately 2. Since the total uncertainty is expected to be statistically-dominated, the second method yields a better prediction and we use this as our estimate of the $t\bar{t}$ background.
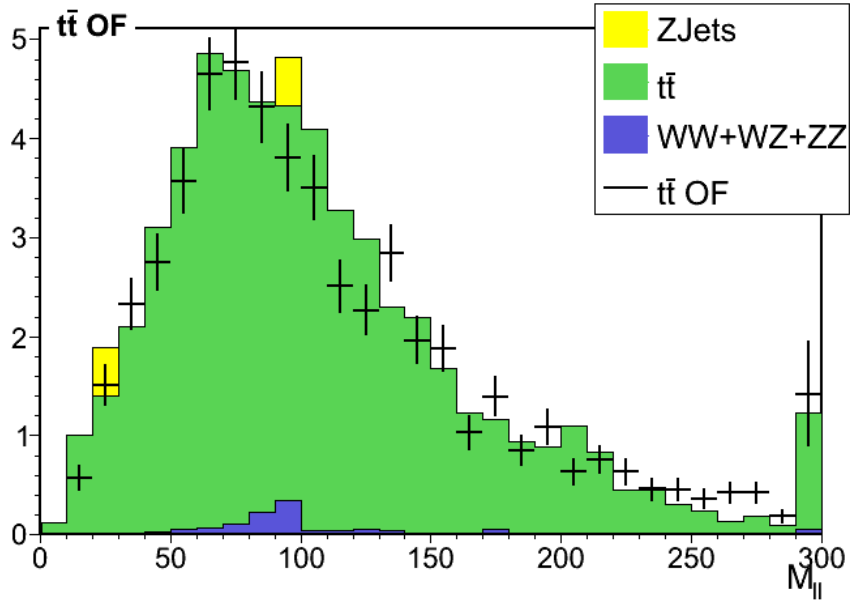


Figure 5: Dilepton mass distribution for events passing the loose signal region selection. The solid histograms represent the yields in the same-flavor final state for each SM contribution, while the solid black line (OFOS) indicates the sum of the MC contributions in the opposite-flavor final state. The $t\bar{t}$ distribution in the same-flavor final state is well-modeled by the OFOS prediction.

# 9    Non $t\bar{t}$ Backgrounds

Backgrounds from pair production of vector bosons and single top can be reliably estimated from Monte Carlo. They are negligible compared to $t\bar{t}$ as shown in Tables 2 and 3.

Backgrounds from fake leptons are negligible due to the requirement of two $P_T > 20$ GeV leptons in the $Z$ mass window, accompanied by jets and large MET.

13

## 10  Results

The data and SM predictions are shown for all events in Fig. 6, and split between the *ee* and *μμ* final states in Fig. 7 and 8. We observe 14 events (7 in each lepton flavor channel) in the loose signal region (MET > 100GeV), compared to a data-driven prediction of 13.6 ± 0.98, which is dominated by the estimated $t\bar{t}$ contribution. For the tight signal region defined by MET > 200GeV, we observe 2 events (both in the *μμ* channel) compared to a data-driven prediction of 1.34 ± 0.33. These uncertainties are statistical only, and systematic uncertainties will be discussed in Sec. 11. We conclude that no excess of signal with respect to the data-driven prediciton is observed.

For display purposes only, we have taken the $t\bar{t}$ MET distribution from MC and normalized it such that the integral for MET>100 GeV matches the data-driven prediction from the OF subtraction.



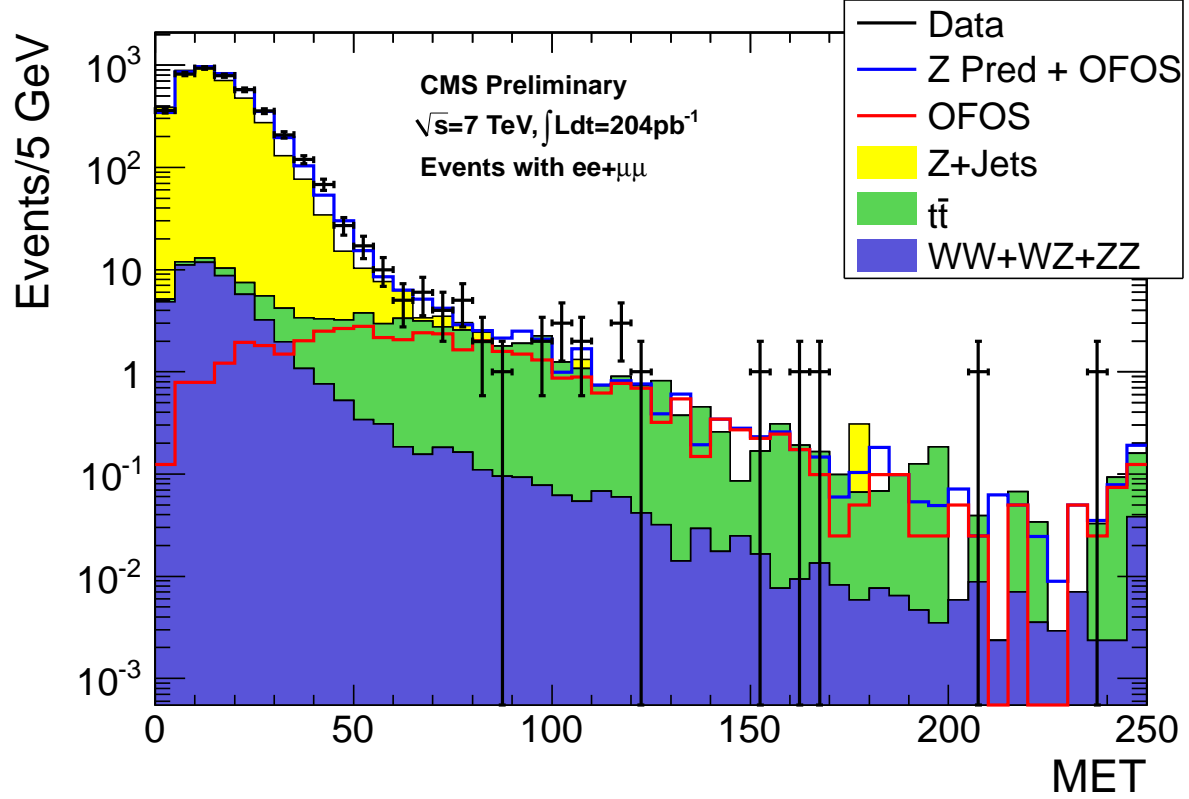|            | N(MET > 30) GeV | N(MET > 60) GeV | N(MET > 100) GeV | N(MET > 200) GeV |
|------------|-----------------|-----------------|------------------|------------------|
| Z pred     | 413.60 ± 1.87   | 15.27 ± 0.19    | 1.84 ± 0.10      | 0.21 ± 0.03      |
| OFOS       | 54.26 ± 2.08    | 34.55 ± 1.66    | 11.76 ± 0.97     | 1.13 ± 0.33      |
| Z pred + OFOS | 467.86 ± 2.77 | 49.82 ± 1.67   | 13.60 ± 0.98     | 1.34 ± 0.33      |
| data       | 484             | 39              | 14               | 2                |

Figure 6: The observed MET distribution for data in the *ee* and *μμ* channels (black points), predicted $t\bar{t}$ MET distribution (red line), the sum of predicted $t\bar{t}$ MET distribution and Z MET distribution predicted from photon MET templates (solid blue line), and MC stacked for dominant backgrounds. Below the plot is tabulated the integral of the predicted MET distribution using the MET templates method (Z pred), the predicted ttbar yield using the opposite flavor subtraction technique (OFOS), the sum of these two contributions (Z pred + OFOS), and the observed MET distribution (data), for MET > 30 GeV and > 60 GeV (which are shown as cross checks), and for the signal regions of MET > 100 GeV and > 200 GeV.

14

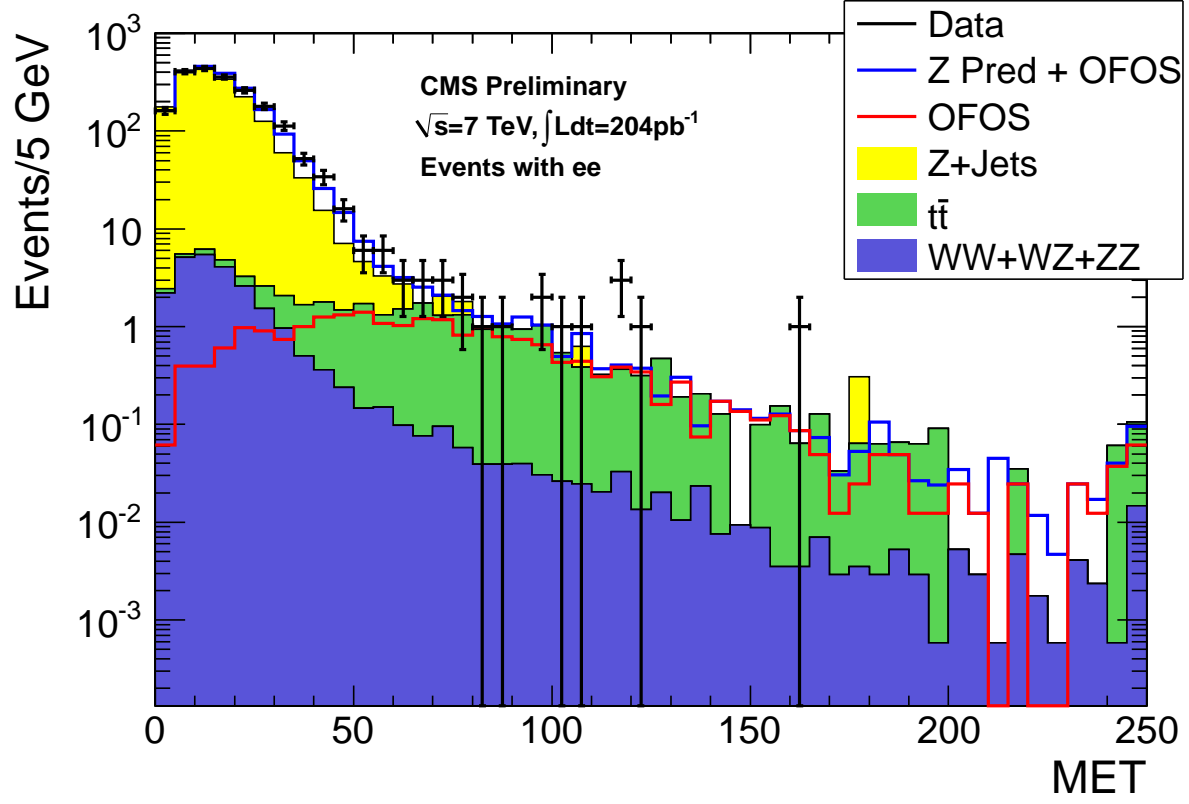| | N(MET > 30) GeV | N(MET > 60) GeV | N(MET > 100) GeV | N(MET > 200) GeV |
|---|---|---|---|---|
| Z pred | 199.58 ± 1.30 | 7.67 ± 0.13 | 0.94 ± 0.07 | 0.12 ± 0.02 |
| OFOS | 25.56 ± 1.38 | 16.28 ± 1.10 | 5.54 ± 0.64 | 0.53 ± 0.22 |
| Z pred + OFOS | 225.14 ± 1.90 | 23.95 ± 1.11 | 6.48 ± 0.64 | 0.65 ± 0.22 |
| data | 247 | 22 | 7 | 0 |

Figure 7: The observed MET distribution for data in the *ee* channels (black points), predicted $t\bar{t}$ MET distribution (red line), the sum of predicted $t\bar{t}$ MET distribution and Z MET distribution predicted from photon MET templates (solid blue line), and MC stacked for dominant backgrounds. Below the plot is tabulated the integral of the predicted MET distribution using the MET templates method (Z pred), the predicted ttbar yield using the opposite flavor subtraction technique (OFOS), the sum of these two contributions (Z pred + OFOS), and the observed MET distribution (data), for MET > 30 GeV and > 60 GeV (which are shown as cross checks), and for the signal regions of MET > 100 GeV and > 200 GeV.
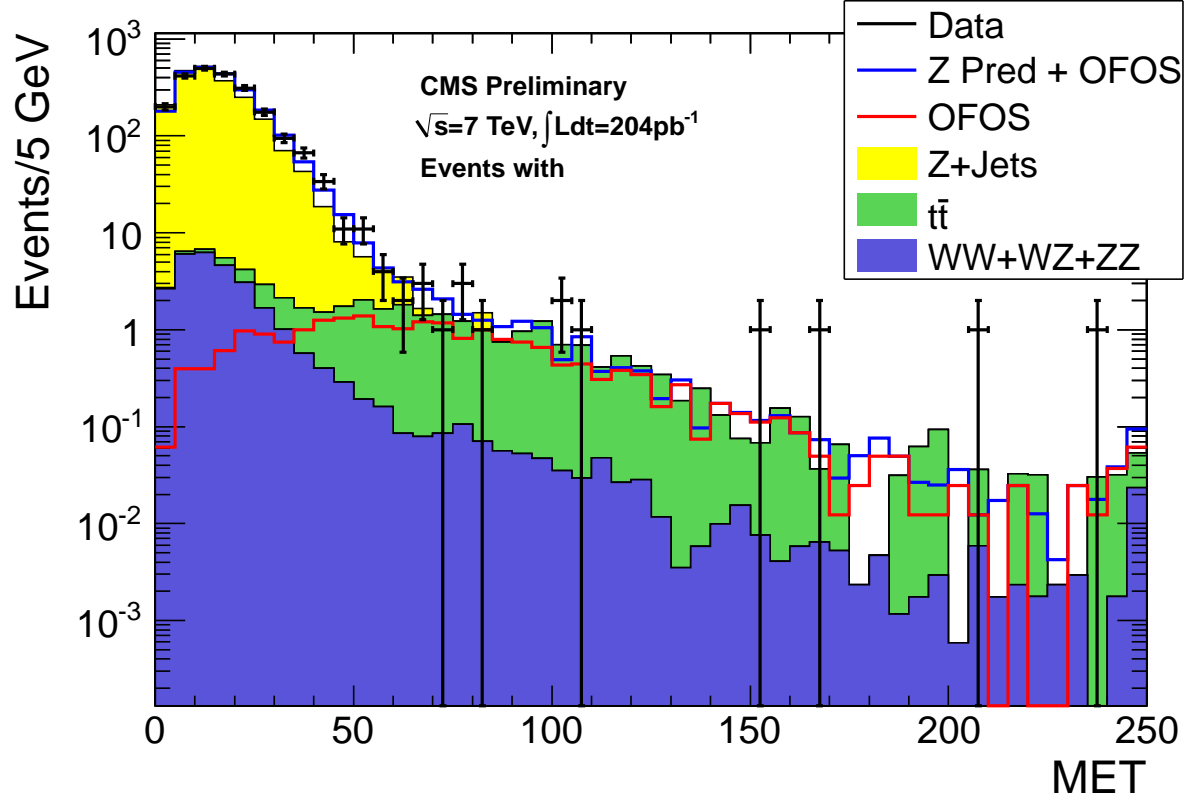
| | N(MET > 30) GeV | N(MET > 60) GeV | N(MET > 100) GeV | N(MET > 200) GeV |
|---|---|---|---|---|
| Z pred | 196.15 ± 1.54 | 6.16 ± 0.09 | 0.65 ± 0.03 | 0.07 ± 0.02 |
| OFOS | 28.70 ± 1.55 | 18.28 ± 1.24 | 6.22 ± 0.72 | 0.60 ± 0.24 |
| Z pred + OFOS | 224.85 ± 2.18 | 24.44 ± 1.24 | 6.87 ± 0.72 | 0.67 ± 0.24 |
| data | 237 | 17 | 7 | 2 |

Figure 8: The observed MET distribution for data in the $\mu\mu$ channels (black points), predicted $t\bar{t}$ MET distribution (red line), the sum of predicted $t\bar{t}$ MET distribution and Z MET distribution predicted from photon MET templates (solid blue line), and MC stacked for dominant backgrounds. Below the plot is tabulated the integral of the predicted MET distribution using the MET templates method (Z pred), the predicted ttbar yield using the opposite flavor subtraction technique (OFOS), the sum of these two contributions (Z pred + OFOS), and the observed MET distribution (data), for MET > 30 GeV and > 60 GeV (which are shown as cross checks), and for the signal regions of MET > 100 GeV and > 200 GeV.

# 11   Systematics Uncertainties in the Background Prediction

We discuss here the sources of uncertainty in the background predictions from the MET templates and OF subtraction methods.

## 11.1   Template Method Related Systematics

In this section, we list several sources of systematic uncertainties related to the template method, as summarized in Table. 4. We perform several variations in the template prediction, and check the corresponding relative difference in the predicted yield for the loose signal region. We have checked that the variations in the predicted yield do not depend strongly on the MET cut, within statistical uncertainties.

Table 4: Summary of variations in the MET templates prediction. The yields predicted by the MET templates method in the loose signal region (MET$> 60$ GeV) are shown, along with the relative difference with respect to the nominal prediction, for several sources of variation in the template prediction.

|  | N(MET$> 60$ GeV) | Rel Diff |
|---|---|---|
| Nominal | $1.81 \pm 0.13$ | |
| nVtx reweighting | $1.79 \pm 0.13$ | -0.01 |
| hadronic recoil $P_T$ reweighting | $2.27 \pm 0.21$ | +0.25 |
| vary photon selection (emf $> 0.8$) | $1.73 \pm 0.17$ | -0.04 |
| vary photon selection (emf $> 0.9$) | $2.27 \pm 0.35$ | +0.25 |
| vary photon selection (h/e $< 0.05$) | $1.52 \pm 0.12$ | -0.16 |
| vary photon selection (h/e $< 0.01$) | $2.18 \pm 0.37$ | +0.20 |

- A difference in $Z$ $P_T$ vs photon $P_T$ introduces a difference in the boost of the hadronic system, which affects the MET distribution due to coherent mismeasurement of the hadronic activity. We test this using a reweighting procedure based on the distribution of the hadronic recoil $P_T$ in the $Z$ and photon samples. We normalize to unit area the distributions of hadronic recoil $P_T$ in the 2 samples, and assess to each photon event a weight which is equal to the ratio of the $Z$ :$P_T$ contributions in the corresponding bin of hadronic recoil $P_T$ . This procedure gives a relative difference of 25% in the predicted yield and we assess a corresponding uncertainty.

- The photon triggers are prescaled as the instantaneous luminosity increased. As a result, the number of pile up events is different in $Z$ events than in photon events, as the latter were preferentially taken at lower instantaneous luminosity. However, this difference is largely compensated because the photon events are weighted by the trigger rescale. We perform the same reweighting procedure using the nVertex distribution in $Z$ and photon events. This procedure gives uncertainties of less than 1%, which we regard as negligible.

- Backgrounds to the photon sample from events where the "photon object" includes hadronic energy that was lost will artificially increase the MET templates. If this was a significant effect, then altering the photon selection ought to significantly change the MET prediction. We test for this by by tightening the cuts on neutral EM fraction and h/e. Based on these studies we assess an uncertainty of 25%

Based on these studies we assess an uncertainty of 25% on the MET templates background prediction, which is entirely dominated by the difference in the $Z$ vs. photon hadronic recoil $P_T$ distributions. We therefore predict the following Z + jets + MET background predictions using the MET templates method:
loose signal region: $1.81 \pm 0.13$ (stat) $\pm 0.45$ (syst)
tight signal region: $0.14 \pm 0.03$ (stat) $\pm 0.04$ (syst).

## 11.2   Systematics of OF Subtraction

The uncertainty on the background prediction from the OF subtraction comes from the uncertainties in 2 quantities: $\epsilon_{e\mu} = \epsilon(e)/\epsilon(\mu)$, the ratio of muon to electron selection efficiencies, and $K$, the fraction of $t\bar{t}$ events which fall inside the $Z$ mass window. The uncertainty in $\epsilon_{e\mu}$ is due to the fact that the efficiencies

are measured in a $Z$ sample and applied to a $t\bar{t}$ sample. In the ttdilepton cross-section measurement the isolation efficiencies are found to vary by 4% per lepton in $Z$ vs. $t\bar{t}$ events. We therefore assess a 5% uncertainty in $\epsilon_{e\mu}$, which is conservative because the difference in isolation efficiency is due to an increase in hadronic activity which is modeled in the MC, and also because $\epsilon_{e\mu}$ is a ratio and the uncertainty partially cancels. The uncertainty in $K$ is due to the uncertainty in the lepton energy scale and is therefore quite small. Varying the boundaries of the $Z$ mass window by $\pm 2$ GeV results in a relative change in $K$ of 2% and we assess a corresponding uncertainty.

Based on these studies we find the following predicted $t\bar{t}$ yields from the OF subtraction technique:

loose signal region: $4.24 \pm 0.82$ (stat) $\pm 0.23$ (syst)

tight signal region: $1.10 \pm 0.42$ (stat) $\pm 0.06$ (syst).

# 12   Upper Limit on Non SM Yield

Summing the predicted backgrounds from the MET templates and OF subtraction gives:

loose signal region: $6.04 \pm 0.82$ (stat) $\pm 0.51$ (syst)

tight signal region: $1.24 \pm 0.42$ (stat) $\pm 0.07$ (syst).

Using these background predictions we calculate the following Bayesian 95% CL upper limits on the non SM event yields (Gaussian nuissance parameter model):

loose signal region: $N_{BG} = 6.04 \pm 0.96$, $N_{OBS} = 7 \rightarrow$ **UL = 7.9 events**

tight signal region: $N_{BG} = 1.24 \pm 0.43$, $N_{OBS} = 0 \rightarrow$ **UL = 3.0 events**


# 13   Additional Information for Model Testing

Other models of new physics in the dilepton final state can be confronted in an approximate way by simple generator-level studies that compare the expected number of events in 34.0 pb$^{-1}$ with our upper limits of 7.9 events (loose signal region) and 3.0 events (tight signal regions). The key ingredients of such studies are the kinematic cuts described in this note, the lepton efficiencies, and the detector response for MET.

The muon identification efficiency is $\approx 92\%$; the electron identification efficiency varies from $\approx 86\%$ at $P_T = 20$ GeV to 93% for $P_T > 50$ GeV (see Fig. 9 top).

The lepton isolation efficiency varies with lepton momentum, as well as the jet activity in the event. In $t\bar{t}$ events, it varies from $\approx 87\%$ (muons) and $\approx 90\%$ (electrons) at $P_T = 20$ GeV to $\approx 95\%$ for $P_T > 60$ GeV. In LM4 (LM8) events, this efficiency is degraded by $\approx 2 - 5\%$ ($\approx 10 - 13\%$) over the whole momentum spectrum (see Fig. 9 bottom).

The average detector response (the reconstructed quantity normalized to the generated quantity) for MET is $0.96 \pm X$ where the uncertainties originate from the hadronic energy scale uncertainty. The experimental resolution on this quantity is 17%.

# 14   Model-Dependent Limits

As an example of how the upper limit presented in Sec. 12 can be used to test if a specific model is excluded, in this section we consider the benchmark SUSY processes LM4 and LM8, which contain $Z$ bosons produced in the cascade decays of SUSY particles. We place upper limits on the quantity $\sigma \times BF \times A$, assuming efficiencies and uncertainties from these processes, and compare them to the expected values of $\sigma \times BF \times A$. Here $\sigma$ is the signal production cross section, $BF$ is the branching fraction to the final state Z + jets + MET and $A$ is the signal acceptance.

The signal event yield $N_{SIG}$ can be expressed as:

$$N_{SIG} = \sigma \times BF \times A \times \epsilon \times \mathcal{L}, \tag{5}$$

and we therefore have:

$$N_{SIG}/(\epsilon \times \mathcal{L}) = \sigma \times BF \times A. \tag{6}$$

Here $\epsilon$ is the signal efficiency and $\mathcal{L}$ is the integrated luminosity. Since we wish to place an upper limit on the quantity $\sigma \times BF \times A$, we must evaluate the quantity $N_{SIG}/(\epsilon \times \mathcal{L})$. Because of the efficiency in the denominator, this upper limit cannot be calculated in an entirely model-independent way; rather, it must be calculated with respect to a specific model. We therefore evaluate the upper limit on $\sigma \times BF \times A$ with respect to $t\bar{t}$, LM4 and LM8. For each process, we must calculate both the efficiency and its uncertainty, as discussed in the following subsections.

## 14.1  Signal Efficiencies

We evaluate the signal efficiencies using MC. To evaluate these efficiencies for our sample processes, we take as our denominator the number of generated events which pass the following selection at the generator level:

- 2 electrons or muons with $p_T > 20$ GeV and $|\eta| < 2.5$,

- Opposite-sign, same-flavor pair with $81 < M(ll) < 101$ GeV,

- Count genjets with $p_T > 30$ GeV, $|\eta| < 2.5$, $\Delta R > 0.4$ from any selected lepton as defined above,

- At least 2 genjets.

For the loose (tight) signal region efficiency, we add to this the requirement genmet$> 60$ (120) GeV. We take as our numerator the number of events passing the above generator-level selection which also pass the signal region selection at reco-level. For the loose (tight) signal region we find efficiencies of 43% (42%), 54% (55% )and 45% (48%) for $t\bar{t}$, LM4 and LM8, respectively. This efficiency is dominated by the dilepton selection efficiency, which varies from $\sim 0.6 - 0.7$ for the chosen processes.

## 14.2  Signal Efficiency Uncertainties

Here we assess systematic uncertainties in the signal efficiencies for our sample processes, from jet/MET, lepton identification, and luminosity uncertainties.

- Jets and MET selection efficiency: we assess this uncertainty by varying the hadronic energy scale by $\pm 5\%$ following the procedure used in the ttdilepton cross-section measurement. For the loose (tight) signal regions we find uncertainties of 9% (23%), 2% (4%), and 2%(4%) for $t\bar{t}$, LM4 and LM8, respectively.

- Lepton ID and isolation efficiencies: we perform a tag-and-probe technique on Z data and MC and find that the simulation agrees with data within about 2% as shown in Table 5. We apply a conservative 5% uncertainty on the dilepton selection efficiency.

- Trigger efficiency: the trigger efficiency is very close to 1 since there are 2 leptons with $P_T > 20$ GeV. We apply the simplified model of the trigger efficiency documented in [1] and assess the uncertainty as the relative difference in the yields between assuming 100% trigger efficiency vs. using the trigger model. This procedure gives differences of less than 1% and the trigger efficiency uncertainty is therefore regarded as negligible.

- Luminosity: we assess an uncertainty of 11%.

## 14.3  Upper Limits on $\sigma \times BF \times A$

Armed with the efficiencies and uncertainties calculated in the previous 2 sections, we proceed to calculate upper limits on the quantity $\sigma \times BF \times A$. We calculate Bayesian 95% CL upper limits using the cl95cms software, assuming a log-normal model of nuissance parameter integration. We also calculate the quantity $\sigma \times BF \times A$ for LM4 and LM8, for which we assume LO cross-sections of 1.88 pb and 0.73 pb and calculate

Table 5: Tag and probe results on $Z \to \ell\ell$ on data and MC. We quote ID efficiency given isolation and the isolation efficiency given ID.

|  | Data T&P | MC T&P |
|---|---|---|
| $\epsilon(id\|iso)$ els | $0.918 \pm 0.003$ | $0.936 \pm 0.0038$ |
| $\epsilon(iso\|id)$ els | $0.986 \pm 0.001$ | $0.987 \pm 0.0018$ |
| $\epsilon(id\|iso)$ mus | $0.962 \pm 0.002$ | $0.964 \pm 0.0027$ |
| $\epsilon(iso\|id)$ mus | $0.987 \pm 0.001$ | $0.984 \pm 0.0018$ |

k-factors for each event, depending on the sub-process. The quantity $BF \times A$ is taken to be the fraction of the total number of generated events which pass the generator-level selection given in Sec. 14.1. The results are summarized in Table 6. These results show that the LM4 and LM8 benchmark points are beyond the sensitivity of this search with the current integrated luminosity.

Table 6: Summary of efficiencies, efficiency uncertainties (quadrature sum of jet/MET, dilepton and luminosity uncertainties), and upper limits on $\sigma \times BF \times A$ for the loose (MET> 60 GeV) and tight (MET> 120 GeV) signal regions. We also show the quantity $\sigma \times BF \times A$ for LM4 and LM8.

|  | $t\bar{t}$ | LM4 | LM8 |
|---|---|---|---|
| **Loose signal region** |  |  |  |
| Efficiency | 0.43 | 0.54 | 0.45 |
| Efficiency Uncertainty | 0.15 | 0.12 | 0.12 |
| UL($\sigma \times BF \times A$) (pb) | 0.56 | 0.44 | 0.53 |
| $\sigma \times BF \times A$ (pb) |  | 0.045 | 0.025 |
| **Tight signal region** |  |  |  |
| Efficiency | 0.42 | 0.55 | 0.48 |
| Efficiency Uncertainty | 0.26 | 0.13 | 0.13 |
| UL($\sigma \times BF \times A$) (pb) | 0.23 | 0.17 | 0.19 |
| $\sigma \times BF \times A$ (pb) |  | 0.035 | 0.018 |

# 15   Conclusion

We have performed a search for BSM physics in the Z + jets + MET final state. Backgrounds from SM Z production were estimated using the data-driven MET templates method, and backgrounds from $t\bar{t}$ were estimated using the data-driven opposite-flavor subtraction technique. We found no evidence for anomalous yield beyond SM expectations and placed Bayesian 95% CL upper limits on the non SM yields in the loose (MET>60 GeV) and tight signal regions (MET>120 GeV), of 7.9 and 3.0 events, respectively. We also quoted upper limits on the quantity $\sigma \times BF \times A$, assuming efficiencies and uncertainties from the benchmark SUSY processes LM4 and LM8.
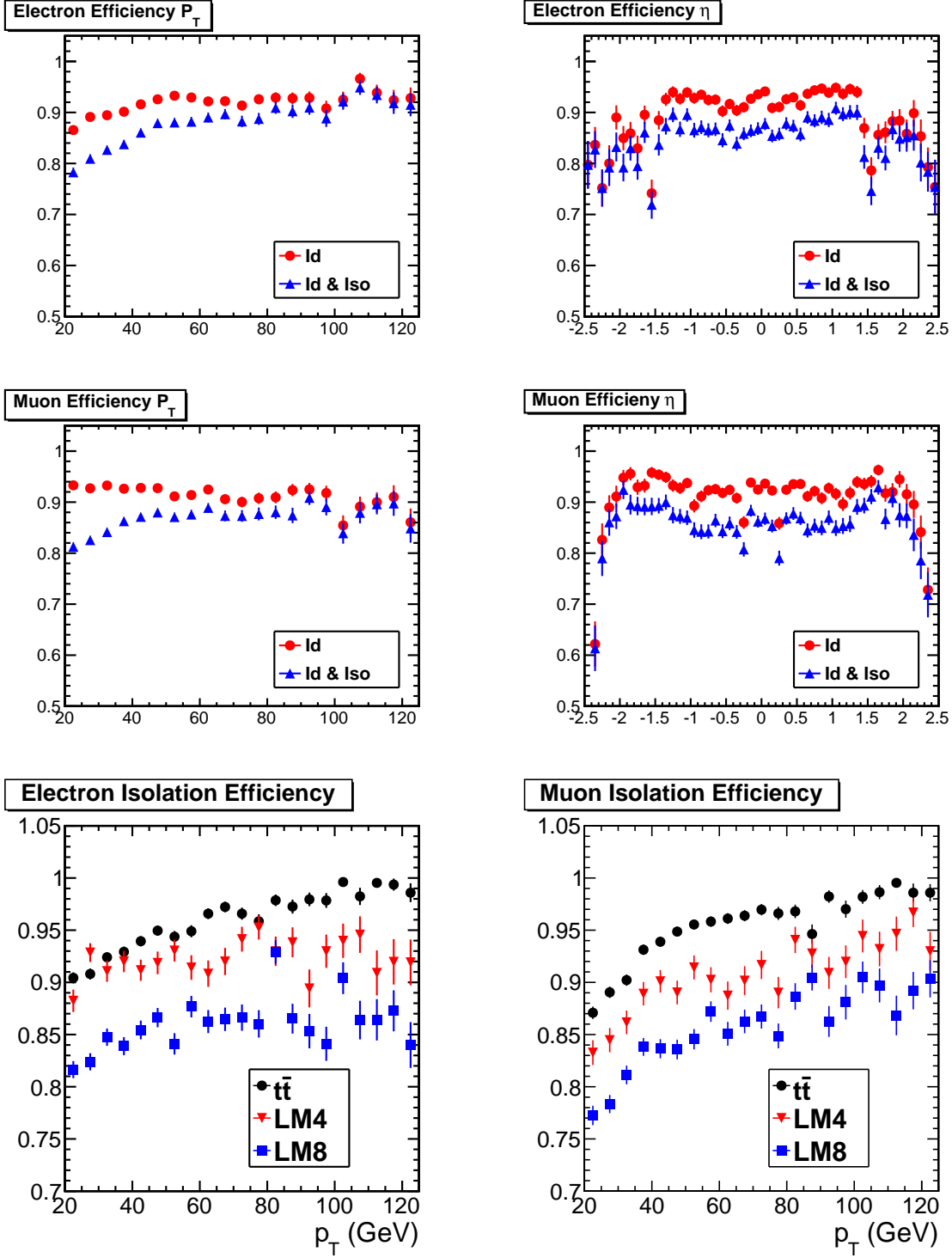
Figure 9: Identification and isolation efficiencies for leptons from $t \to W \to \ell$ and $t \to W \to \tau \to \ell$ in $t\bar{t}$ events (top). Isolation efficiency for $t\bar{t}$, LM4 and LM8 (bottom).
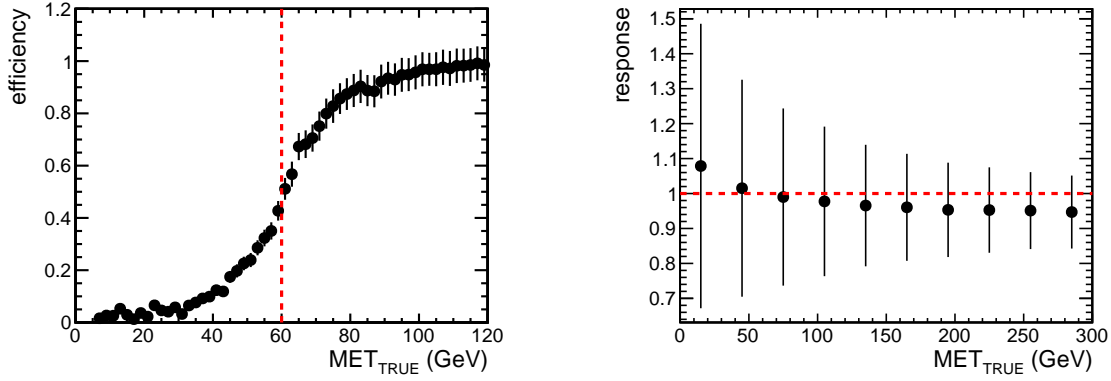
Figure 10: Left: the efficiency to pass the MET > 60 GeV requirement (indicated by the vertical dashed line) as a function of the true MET. Right: the average detector response (reconstructed MET divided by true MET) and its RMS, as a function of true MET. These plots are made with LM4 MC, but they are not expected to depend strongly on the underlying physics.

# References

[1] arXiv:1103.1348v1, [2011 note]

[2] V. Pavlunin, Phys. Rev. **D81**, 035005 (2010).

[3] V. Pavlunin, CMS AN-2009/125

[4] A reference to the top paper, once it is submitted. Also D. Barge *et al.*, AN-CMS2010/258.

[5] Changes to the selection for the 38x CMSSW release are given in
    `https://twiki.cern.ch/twiki/bin/viewauth/CMS/TopDileptonRefAnalysis2010Pass5`.

[6] https://twiki.cern.ch/twiki/bin/viewauth/CMS/SimpleCutBasedEleID

[7] https://twiki.cern.ch/twiki/bin/viewauth/CMS/EgammaWorkingPointsv3

[8] D. Barge *at al.*, AN-CMS2009/159.

[9] B. Mangano *et al.*, AN-CMS2010/283.

[10] https://twiki.cern.ch/twiki/bin/viewauth/CMS/CrossSections_3XSeries,
    https://twiki.cern.ch/twiki/bin/view/CMS/ProductionSpring2011

[11] D. Barge *at al.*, AN-CMS2009/130.

[12] W. Andrews *et al.*, AN-CMS2009/023.

[13] D. Barge *at al.*, AN-CMS2010/257.

# A Triggers

## A.1 Dilepton Triggers

The detailed list of triggers for selecting dilepton events is (with the version number omitted for simplicity):

- double-muon triggers
  - `HLT_DoubleMu7_v`
  - `HLT_Mu13_Mu7_v`
- double-electron triggers
  - `HLT_Ele17_CaloIdL_CaloIsoVL_Ele8_CaloIdL_CaloIsoVL_v`
  - `HLT_Ele17_CaloIdT_TrkIdVL_CaloIsoVL_TrkIsoVL_Ele8_CaloIdT_TrkIdVL_CaloIsoVL_TrkIsoV`
- e-$\mu$ cross triggers
  - `HLT_Mu17_Ele8_CaloIdL_v`
  - `HLT_Mu8_Ele17_CaloIdL_v`

## A.2 Photon Triggers

The photon triggers used are:

- `HLT_Photon20_CaloIdVL_IsoL_v*`
- `HLT_Photon30_CaloIdVL_IsoL_v*`
- `HLT_Photon50_CaloIdVL_IsoL_v*`
- `HLT_Photon75_CaloIdVL_IsoL_v*`

The HLT requirements on the above triggers are [7]:

- CaloIdVL:
  H/E < 0.15 (0.1), $\sigma_{i\eta i\eta} < 0.024$ (0.04) in barrel (endcap)
- IsoL:
  Ecal ET < 5.5 + 0.012*ET, Hcal ET < 3.5 + 0.005*ET, Trk PT < 3.5 + 0.002*ET

# B MET Templates from Photon Sample

In this appendix we display our templates derived from the photon sample using the HLTPhoton20 (Fig. 11), HLTPhoton30 (Fig. 12), HLTPhoton50 (Fig. 13) and HLTPhoton70 (Fig. 14) triggers.
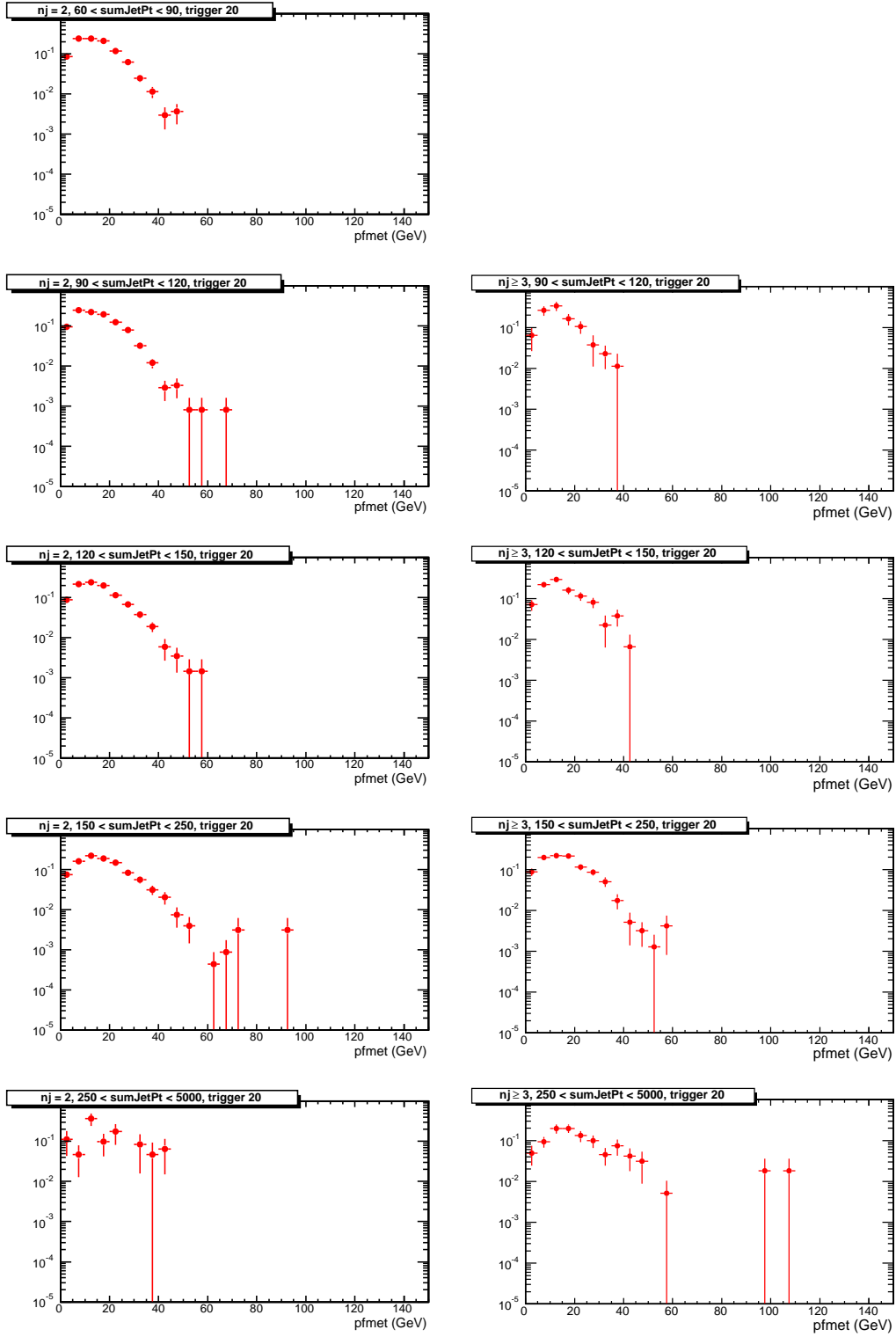
Figure 11: MET Templates derived from the HLTPhoton20 sample.
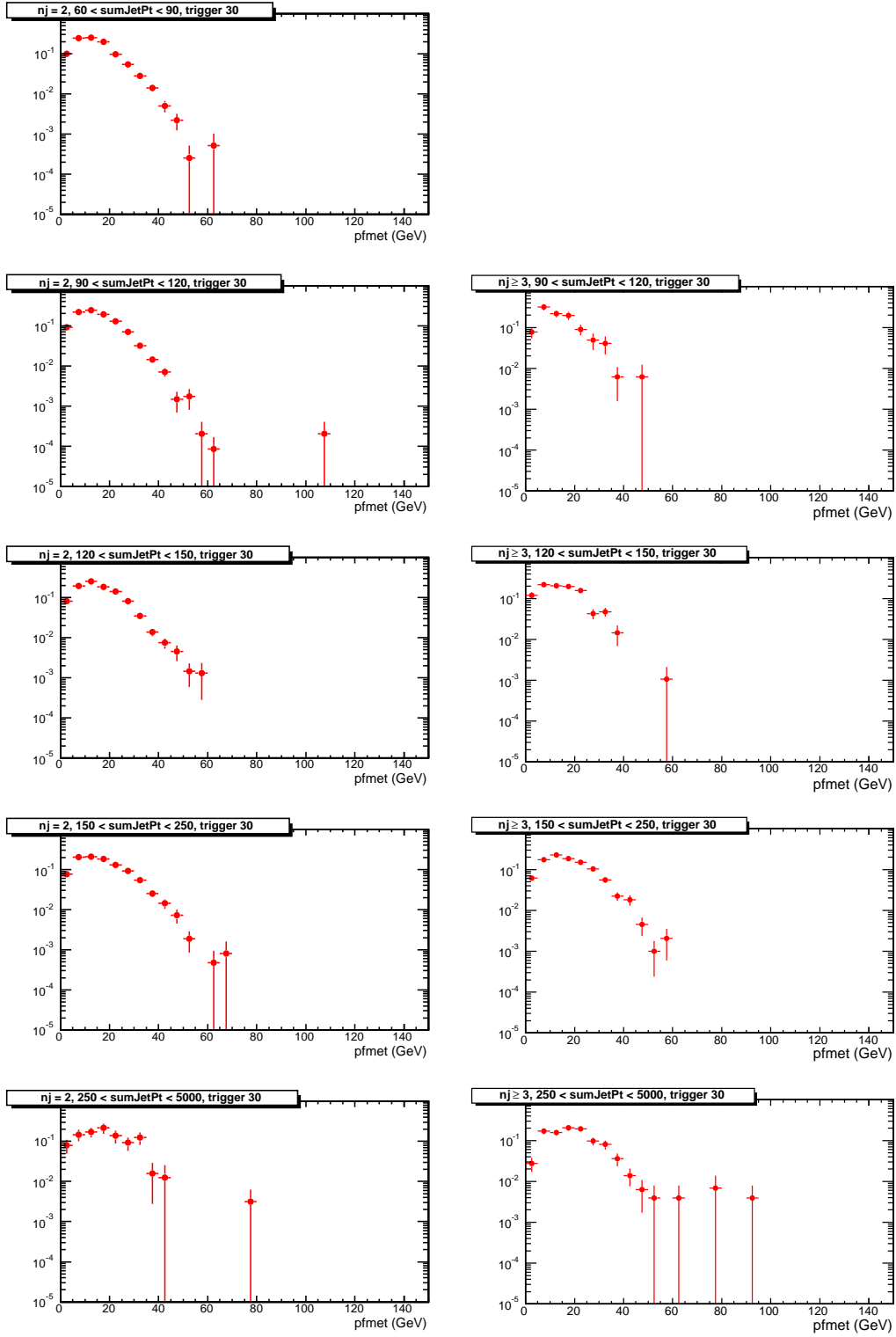
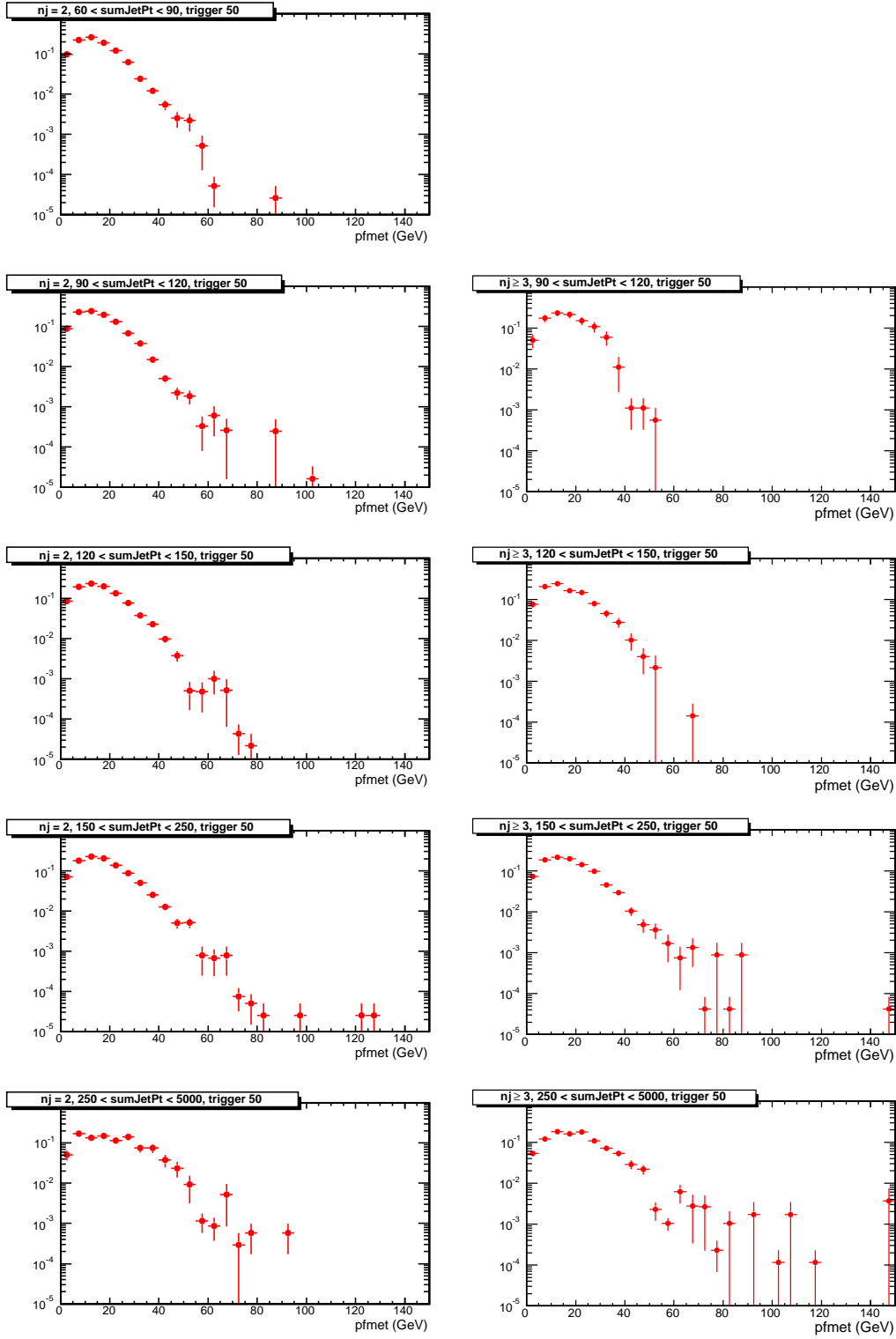Figure 12: MET Templates derived from the HLTPhoton30 sample.
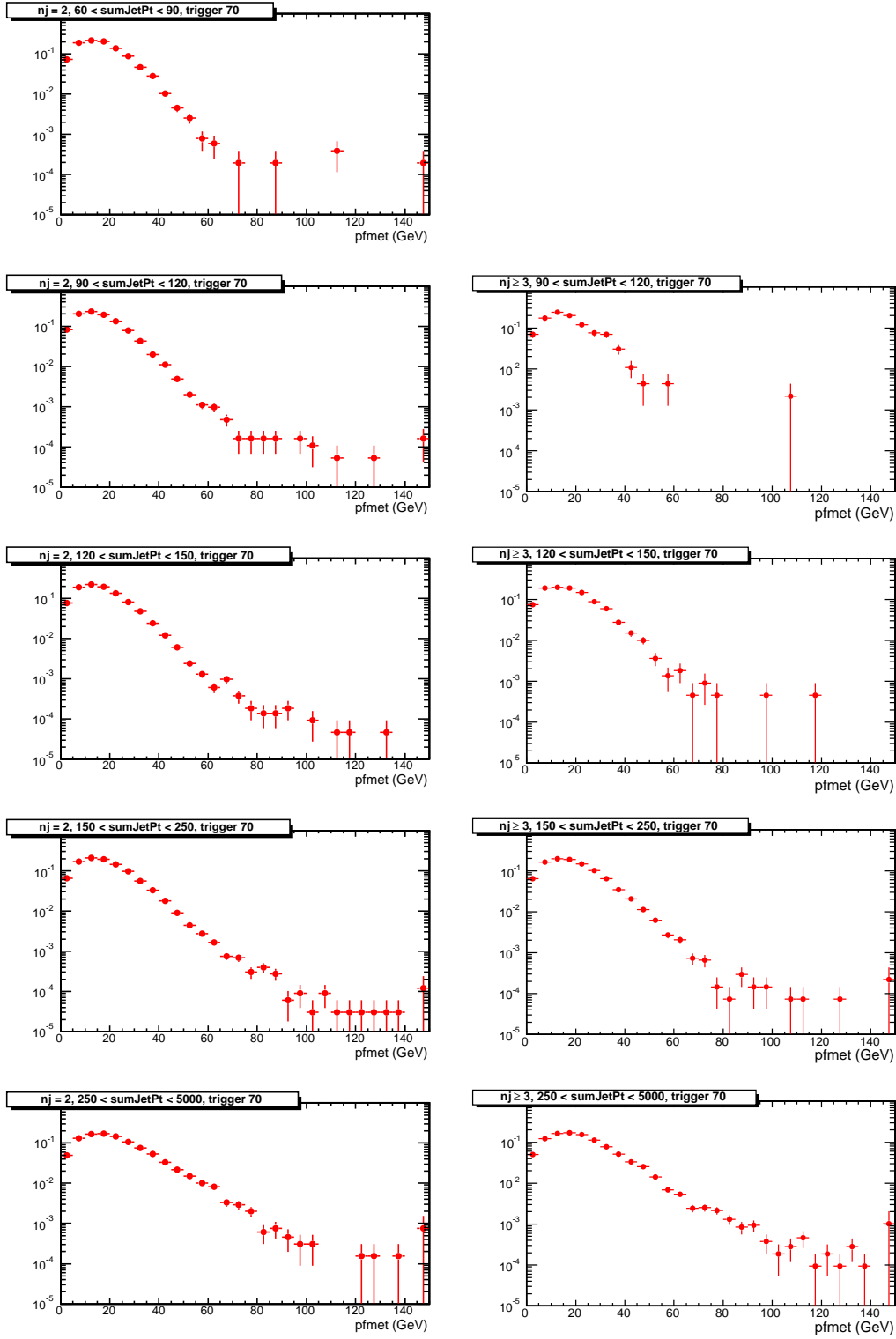
Figure 13: MET Templates derived from the HLTPhoton50 sample.

Figure 14: MET Templates derived from the HLTPhoton70 sample.